Manuscript prepared for Nat. Hazards Earth Syst. Sci.
with version 2014/09/16 7.15 Copernicus papers of the LaTeX class copernicus.cls.
Date: 27 June 2017

Supporting material - Simple and approximate estimation of future precipitation return-values

Rasmus E. Benestad[1], Kajsa M. Parding[1], Abdelkader Mezghani[1], and Anita V. Dyrrdal[1]

[1]The Norwegian Meteorological Institute, Henrik Mohns Plass 1, Oslo, 0313, Norway

Correspondence to: Rasmus E. Benestad (rasmus.benestad@met.no)

Abstract. This supporting material provides additional analyses that addresses some of the assumptions made in the main paper. It also explains the strategy that we chose and to emphasise this has been structured as questions and answers. The analysis presented here was carried out with the open source R-package 'esd' (Benestad et al., 2015). An R-markdown script with the step-by-step code of the analysis is available from figshare.com for the sake of traceability and replicability (DOI: 10.6084/m9.figshare.4476419)

1 Is the wet-day frequency stationary?

In this paper, we estimate future return-values of precipitation based on temperature projections, but neglect to evaluate changes in the wet-day frequency (f_w) and simply assume it to be stationary. How does this assumption hold up? Has the wet-day frequency varied significantly in the past and do we expect large changes in the future? To answer these questions we have studied the seasonal cycle and past trends of the wet-day frequency.

Changes in the wet-day frequency affect the probability for heavy precipitation amounts in the future according to $Pr(X > x) = f_w \ e^{-x/\mu}$, and hence influence future return-values according to $x_{1yr} = \mu \ln(365.25 \times f_w)$. This goes for both long-term changes (trends) as well as interannual to decadal variations. Historical precipitation observations can be used to estimate the interannual variability of f_w and its effect on x_{1yr}, but short records mean that the sample size is limited and may preclude a complete account of the effect of decadal changes.

The wet-day frequency responds weakly to the seasonally varying conditions (Figure S3; grey curve), which suggests that it is not too sensitive to systematic changes in the state of the local environment. We can also make use of some information from past trends in the wet-day frequency, as

climate change is already happening (Figures S8 and S9). Historical data suggest different tendencies in different regions (Figure S9), and previous analysis indicates that the wet-day frequency is strongly influenced by the circulation patterns (Benestad and Mezghani, 2015). The analysis of historical precipitation records over the period 1961-2014 show little trend in f_w when taking the mean over all locations (Figure S8), and the only clear spatial pattern is an increase over southern Norway (Figure S9). This should be compared to the wet-day mean precipitation μ which for most of the sites increased during the same period, typically by the order of 0.1 mm/day per decade (Figures S6 and S7).

2 Does variation in the wet-day mean precipitation really correspond to changing probabilities?

The probability framework adopted here can be formulated as $Pr(X < x|\mu)$, meaning that it is conditional on the sample mean of μ and that the distribution is exponential. Previous studies have found that the wet-day daily precipitation is approximately exponentially distributed (Benestad and Mezghani, 2015; Benestad et al., 2012b; Benestad, 2007; Benestad et al., 2012a), albeit with a systematic bias connected to the location. The assumption can be assessed by comparing the actual percentiles with quantiles estimated for different samples with different annual mean μ using the formula for exponentially distributed data:

$$q_p = -ln(1-p)\mu. \tag{SM1}$$

The exponential distribution implies a similar proportional change for all percentiles, which is roughly consistent with a near-constant ratio of increase in daily precipitation percentiles above the 90^{th} percentage (Pall et al., 2007). The two quantities should be similar (as Figure S1 indicates) and the data scattered along the diagonal in a scatter plot, indicating that a high percentile associated with a low wet-day mean μ is consistent with a more moderate percentile for a sample with a higher wet-day mean value.

3 Why use the $100°W - 30°E/0°N - 40°N$ region of the North Atlantic as predictor?

The choice of predictor region (Figure S2) in this study was motivated by the idea that the North Atlantic ocean is an important moisture source for precipitation over Europe and prevailing winds suggest that the moisture is transported from the west. Also, the sea surface temperature is highest at low latitudes, which suggest the highest evaporation closer to the equator. The analysis presented here suggests a good match between the seasonal variations of the temperature averaged over this region and the local wet-day mean (see Figure 1 of the main manuscript). The predictor was defined

as the area mean saturation vapour pressure and the domain was set after some trials for a few stations, but this crude trial did not involve any systematic study nor any type of fitting/tuning.

4 Why use the saturation vapour pressure as predictor and not the temperature?

It is often wise to make use of terms with similar physical dimensions when calibrating statistical models (Benestad et al., 2008). The saturation vapour pressure is proportional to the vapour density (ideal gas law: $e_s = \rho R_s T$), and the total mass is the product between volume and density. The saturation vapour pressure is expected to be more linearly related to the wet-day mean precipitation than temperature because their physical dimensions both involve a measure of the water mass. If temperature was used, on the other hand, then the relationship would be expected to be nonlinear due to the Clausius-Clapeyron equation ($e_s = 10^{(11.40-2353/T)}$ where T is the temperature in Kelvin).

How representative is the exponential distribution for the probabilities associated with heavy precipitation? The exponential distribution is a simple form for the gamma distribution and has only one parameter μ determining its shape as opposed two (location and scale) which gives more freedom in the data-fit. None of these, however, are normally used for the estimation of return-periods and general extreme value (GEV) or generalized Pareto distributions usually used to fit the upper tail of the distribution for stationary data where the shape of the PDF does not change. In the non-stationary case, the small sample represented by the upper tail may not provide the best information in terms of the calibration of a changing PDF over time. Since the area under the curve is always unity (probabilities always add up to one), the upper tail is constrained by the rest of the PDF. An approximate way to tackle the changes is therefore to make use of the bulk of the PDF (Benestad and Mezghani, 2015).

5 Why use the seasonal cycle for model calibration?

Precipitation is generated by different atmospheric processes and depends on many factors. Hence the signal-to-noise ratio is often low for traditional model calibration based on chronological matching between the amount and some large scale variable such as regional temperature.

One technique commonly used in physics and electronics for optimising the information from systems and measurements with low signal-to-noise ratio involves cycles with well-established frequencies (eg. FM in radio, phase-locking), and in meteorology/climatology seasonal variations is the most pronounced cycle. There has also been some analysis of tropical cyclone frequencies based on the seasonal variations (Benestad, 2009), but there is an important caveat associated with such studies: the seasonal variations in the local insolation may affect both the large scale conditions and the local variable under investigation, and their correlation may reflect the common dependency on this forcing rather than common link. Thus, the assumption that the seasonal cycle in the temperature over the North Atlantic is linked with the seasonal precipitation statistics is the weakest point

of this study if one interprets the results as the most likely estimate of the wet-day mean precipitation. Nevertheless, from a physics perspective, it is expected that higher temperatures result in higher evaporation and higher humidity, hence, an increased capacity for greater rainfall amounts. We use the link between the seasonal cycles of μ and e_s to estimate an upper limit of the effect of a change in temperature on the precipitation, rather than the most likely estimate of the wet-day mean precipitation itself. Calculating a climatological seasonal cycle gives a larger sample size compared to analyses applied on individual years, and gives a value that is based on a sample stretching over longer time periods. Calibration on larger sample sizes stretching over longer time periods puts more weight on slow processes with long time scales.

The link between the seasonal cycles of local μ and the mean e_s over the predictor domain (Figure S2) was first assessed by the R^2 of the regression. Figure S5 shows a histogram of the R^2 scores, most of which have an explained variance of over 60%. The majority of the stations with poor fits are found in the mountainous parts of western Norway and the Alps (the size of the markers in Figure 3 of the main manuscript are proportional to R^2), which indicates that the method proposed here does not work in regions with predominantly orographic precipitation.

A second level of validation was to compare trends of historical observations of μ to predicted trends of $\hat{\mu}$ (the seasonal cycle downscaling model applied to the annual mean e_s calculated from NCEP reanalysis temperature data). Figure S6 shows that there is a more pronounced scatter in the observed trends than the predicted trends, which indicates that factors other than the sea surface temperature, that are not captured by the climatological downscaling model, also have influenced the long-term changes.

The link between the wet-day mean precipitation and temperature is also assessed by extending the analysis to the spatial as well as the temporal dimension. The fact that this relationship exists in two different dimensions is a stronger indicator of a physical link than if it were to be limited to only one. Figure S10 shows a scatter plot between e_s and μ calculated based on the local mean daily maximum temperature and precipitation, respectively. The fitted line shows the regression between the local seasonal cycles of μ and the temperature for 1420 locations (CLARIS data) in South America, Europe (stations selected for the COST-VALUE experiment 1), and the US (GDCN). The analysis indicates that the wet-day mean (y-axis) increases by 0.4 mm/day per degree C (x-axis) increase of the local temperature if the elevation is accounted for. The coefficient of the spatial regression is generally consistent with the coefficients from the regressions based on the seasonal cycles, within the range of estimated error margins (Figure S11). An exception was seen in stations located in western Norway and south of the Alps, where the seasonal cycle regression also showed a weak relationship between μ and e_s. It is not expected that the results should be identical, as the climatological temperature involves the mean of the local daily maximum temperature from the stations, whereas the seasonal temperatures were taken from a large region of the ocean and represented daily mean temperature. Nevertheless, similar values for the regression coefficients between e_s and μ supports

the hypothesis that the precipitation amounts are linked to temperature in a way that gives similar changes through the seasonal variations as in spatial variations.

6 Is the model ensemble spread a good proxy for probabilities?

Model ensembles do not really provide estimates of probabilities because they cannot be considered as a random sample of data and because they do not give a perfect reproduction of the observed quantities. According to the IPCC "Ensemble members may not represent estimates of the climate system behaviour (trajectory) entirely independent of one another. This is likely true of members that simply represent different versions of the same model or use the same initial conditions. But even different models may share components and choices of parameterisations of processes and may have been calibrated using the same data sets. There is currently no 'best practice' approach to the characterization and combination of inter-dependent ensemble members, in fact there is no straight forward or unique way to characterize model dependence" (Knutti et al., 2010). Nevertheless, the spread of downscaled annual mean temperature from ensemble experiments such as CMIP5 is often comparable to the magnitude of the observed year-to-year temperature variations(Benestad et al., 2016), and the 95th percentile has been used as an approximate estimate of a one-in-twenty year hot summer season (Benestad, 2011). For all intents and purposes, we have used the interval of the ensembles (see, e.g., Figure S4) as a measure of the variations of the climate system (Deser et al., 2012).

References

Benestad, R.: Novel Methods for Inferring Future Changes in Extreme Rainfall over Northern Europe, Climate Research, 34, 195–210, 2007.

Benestad, R., Nychka, D., and Mearns, L. O.: Spatially and temporally consistent prediction of heavy precipitation from mean values, Nature Climate Change, 2, 544–547, 2012a.

Benestad, R., Nychka, D., and Mearns, L. O.: Specification of wet-day daily rainfall quantiles from the mean value, Tellus A, 64, doi:10.3402/tellusa.v64i0.14981, 2012b.

Benestad, R. E.: On tropical cyclone frequency and the warm pool area, Natural Hazards and Earth System Science, 9, 635–645, doi:10.5194/nhess-9-635-2009, http://www.nat-hazards-earth-syst-sci.net/9/635/2009/, 2009.

Benestad, R. E.: New Evidence of an Enhanced Greenhouse Effect, arXiv preprint arXiv:1106.4937, 2011.

Benestad, R. E. and Mezghani, A.: On downscaling probabilities for heavy 24-hour precipitation events at seasonal-to-decadal scales, Tellus A, 67, doi:10.3402/tellusa.v67.25954, http://www.tellusa.net/index.php/tellusa/article/view/25954, 2015.

Benestad, R. E., Hanssen-Bauer, I., and Chen, D.: Empirical-statistical downscaling, World Scientific, 2008.

Benestad, R. E., Mezghani, A., and Parding, K. M.: esd V1.0, http://dx.doi.org/10.5281/zenodo.29385, 2015.

Benestad, R. E., Parding, K. M., Isaksen, K., and Mezghani, A.: Climate change and projections for the Barents region: what is expected to change and what will stay the same?, Environmental Research Letters, 11, 054 017, doi:10.1088/1748-9326/11/5/054017, http://stacks.iop.org/1748-9326/11/i=5/a=054017, 2016.

Deser, C., Knutti, R., Solomon, S., and Phillips, A. S.: Communication of the role of natural variability in future North American climate, Nature Climate Change, 2, 775–779, 2012.

Knutti, R., Abramowitz, G., Collins, M., Eyring, V., Gleckler, P. J., Hewitson, B., and Mearns, L.: Meeting Report of the Intergovernmental Panel on Climate Change Expert Meeting on Assessing and Combining Multi Model Climate Projections, IPCC Working Group I Technical Support Unit, University of Bern, Bern, Switzerland, 2010.

Pall, P., Allen, M. R., and Stone, D. A.: Testing the Clausius–Clapeyron constraint on changes in extreme precipitation under CO2 warming, Climate Dynamics, 28, 351–363, doi:10.1007/s00382-006-0180-2, http://link.springer.com/10.1007/s00382-006-0180-2, 2007.

Smith, K., Strong, C., and Wang, S.-Y.: Connectivity between Historical Great Basin Precipitation and Pacific Ocean Variability: A CMIP5 Model Evaluation, Journal of Climate, 28, 6096–6112, doi:10.1175/JCLI-D-14-00488.1, http://journals.ametsoc.org/doi/10.1175/JCLI-D-14-00488.1, 2015.

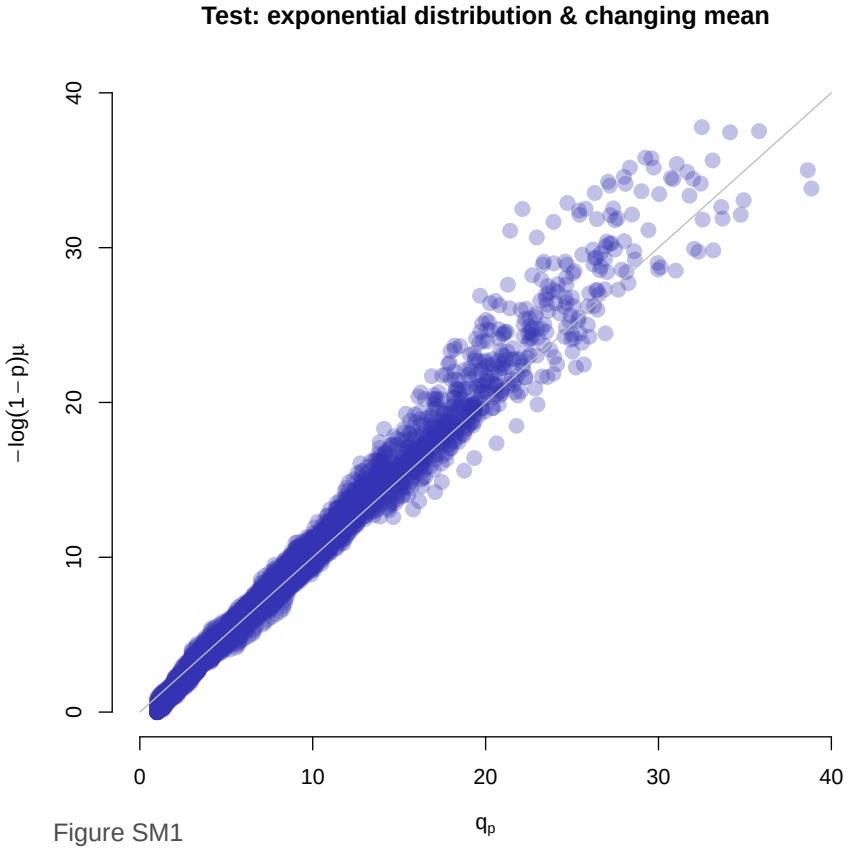

Figure S1. Test for assessing the consistency between the percentiles taken from observations and estimated values using $q_p = -\ln(1-p)\ \mu$ where the values of q_p are estimated using different values of p to compensate for variations in annual mean μ. A critical threshold x can correspond to different percentiles according to $x = q_{p1} = -\ln(1-p1)\ \mu_1 = q_{p2} = -\ln(1-p2)\ \mu_2$.

Figure SM2

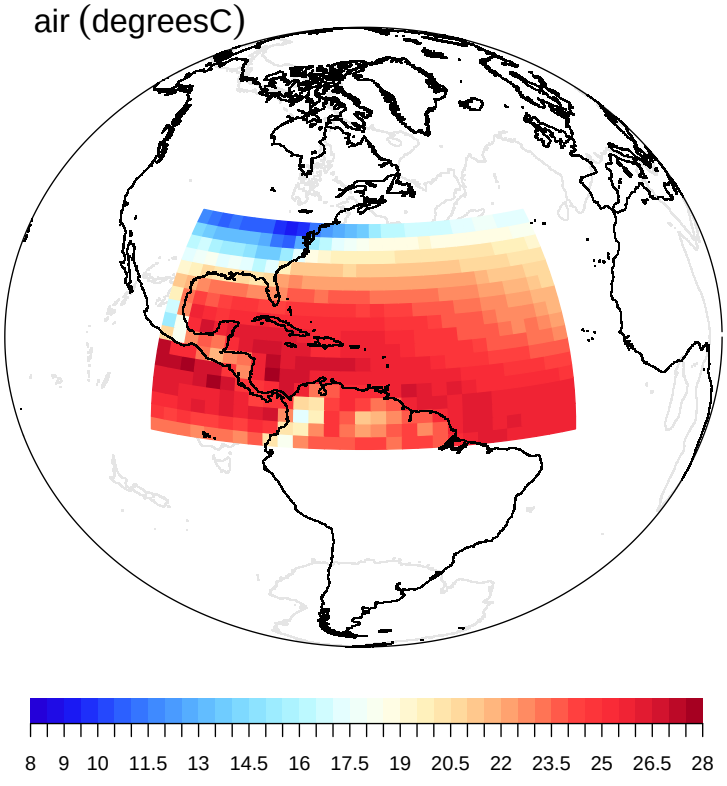

Figure S2. The mean air temperature at 2m of the NCEP reanalysis data set over the chosen predictor domain $100^{\circ}W$-$30^{\circ}E$/$0^{\circ}N$-$40^{\circ}N$.

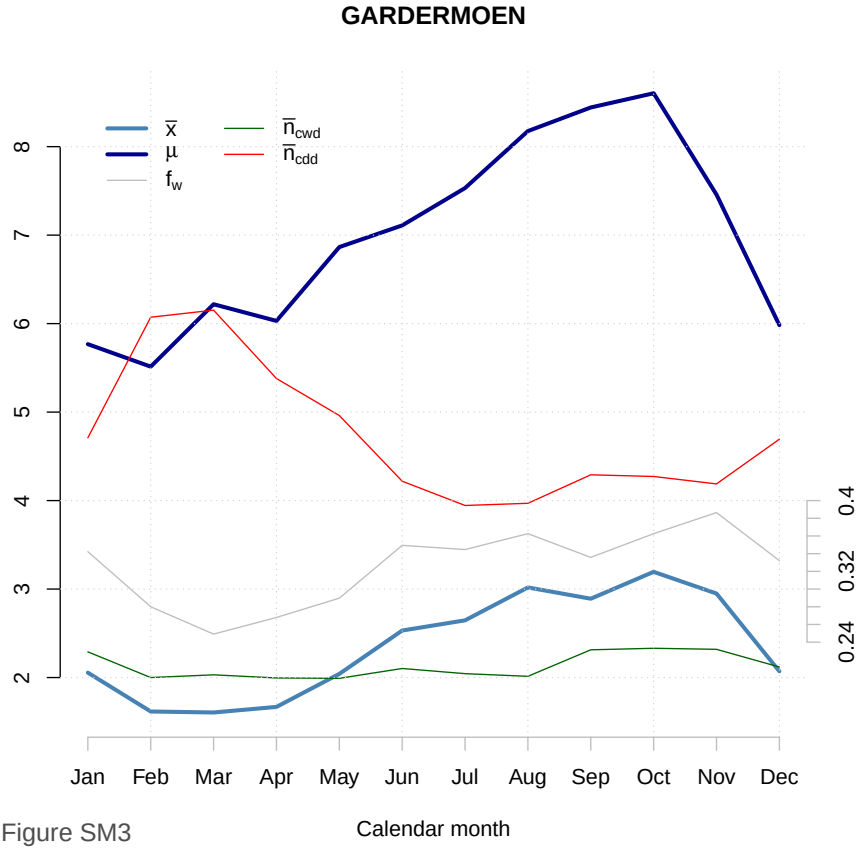

Figure SM3

Figure S3. A comparison between the seasonal cycle in the mean precipitation, the wet-day mean precipitation, the wet-day frequency, as well as the wet and dry spell lengths for a single selected station. The most pronounced seasonal variations tends to be associated with the wet-day mean rather than the mean precipitation or the wet-day frequency.

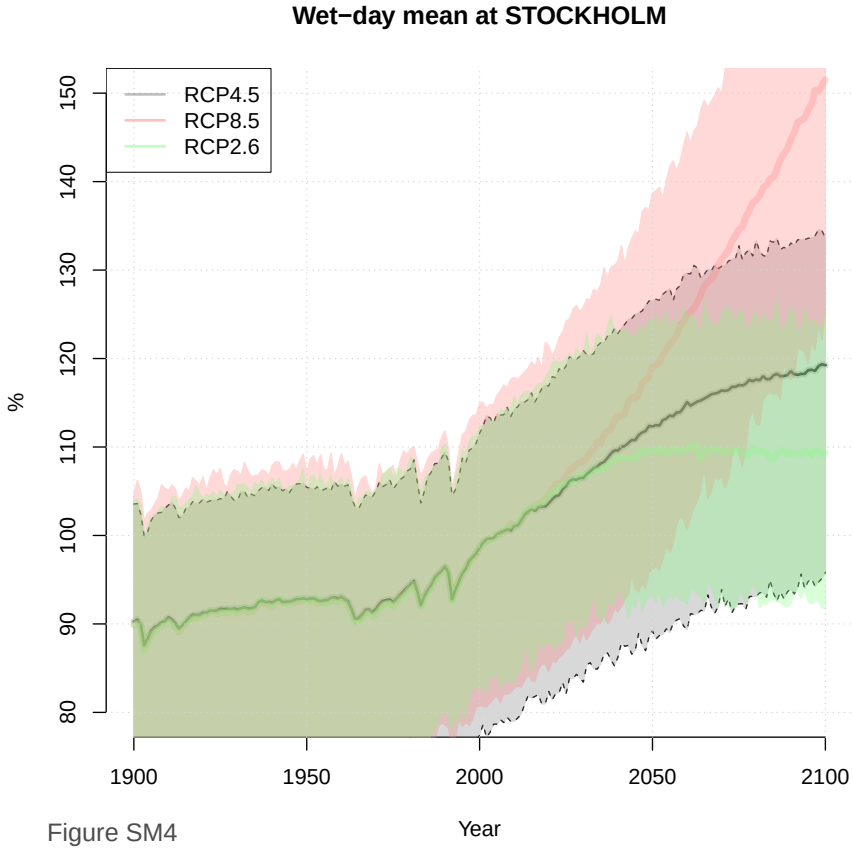

Figure S4. An example of projected annual wet-day mean precipitation μ for the three different emission scenarios RCP 4.5 (grey), RCP2.6 (green) and RCP8.5 (red), expressed as the relative change in comparison to the 2010 values (see Table 1).

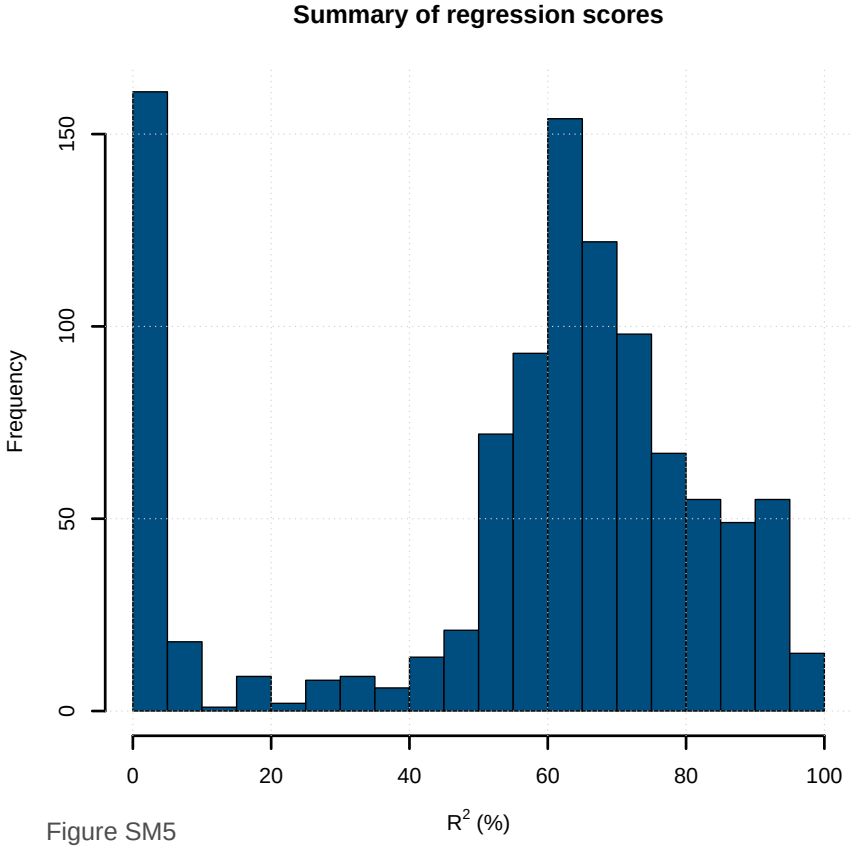

Figure S5. The statistics of the R^2 from the regression between the seasonal cycles in the the local wet-day mean μ and the regionally averaged saturation vapour pressure e_s, estimated from the temperature over the seasonal cycles of the surface temperature over the North Atlantic domain ($100^\circ W$-$30^\circ E$/$0^\circ N$-$40^\circ N$; Figure S2). There is a portion of stations with very low R^2 scores, but most stations suggest an explained variance exceeding 60%.

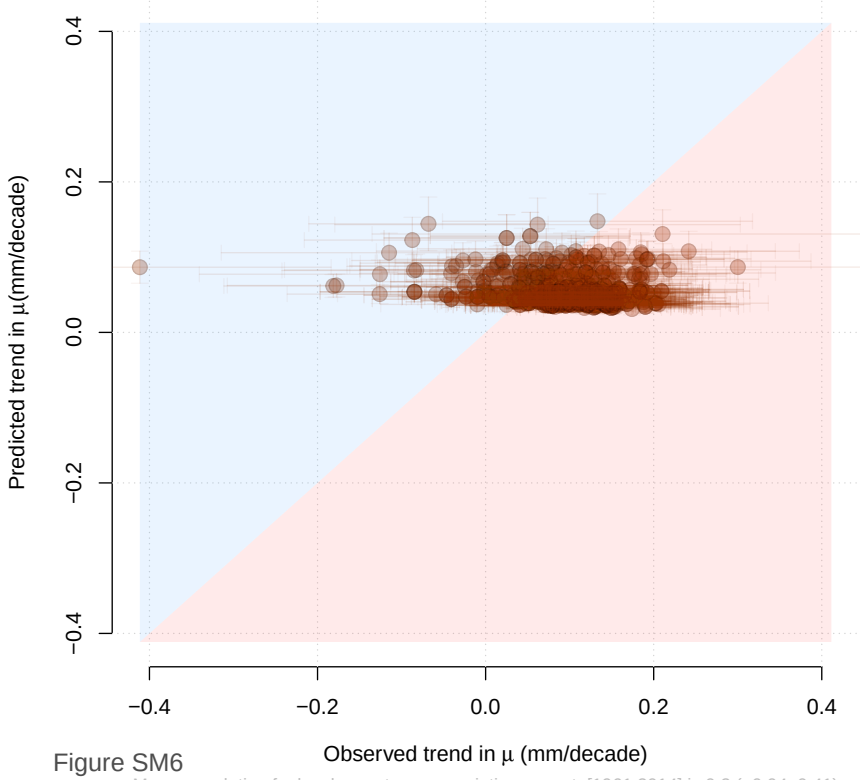

Figure S6. A comparison between the long-term linear trends estimated from the observed annual mean μ and $\hat{\mu}$ values estimated with Equation 1 (see main manuscript) using the saturation water vapor e_s calculated from the NCEP temperature over the North Atlantic domain ($100^\circ W$-$30^\circ E$/$0^\circ N$-$40^\circ N$; Figure S2). The scatter in the observed trends is greater than in the predicted ones, which is consistent with the wet-day mean also being affected by factors other than e_s.

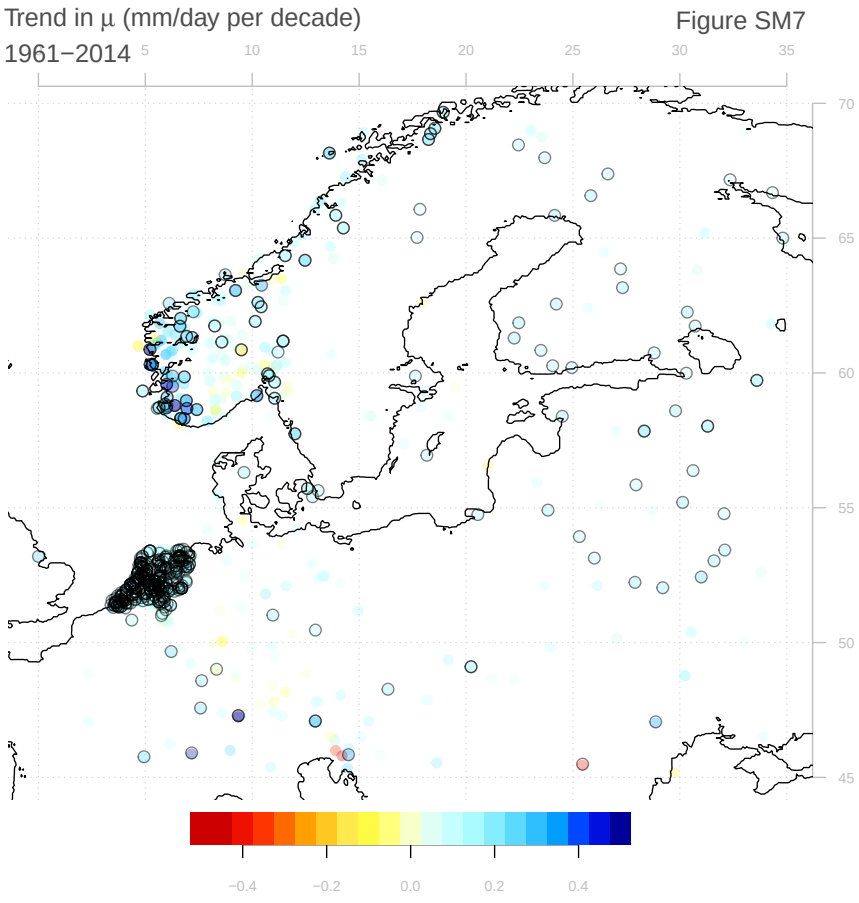

Figure S7. Map of the historical trends in the wet-day mean μ in the period 1961-2014. The trend is generally increasing, but there are a few stations showing a decrease. These outliers are probably spurious, as they do not match the bulk of the data.

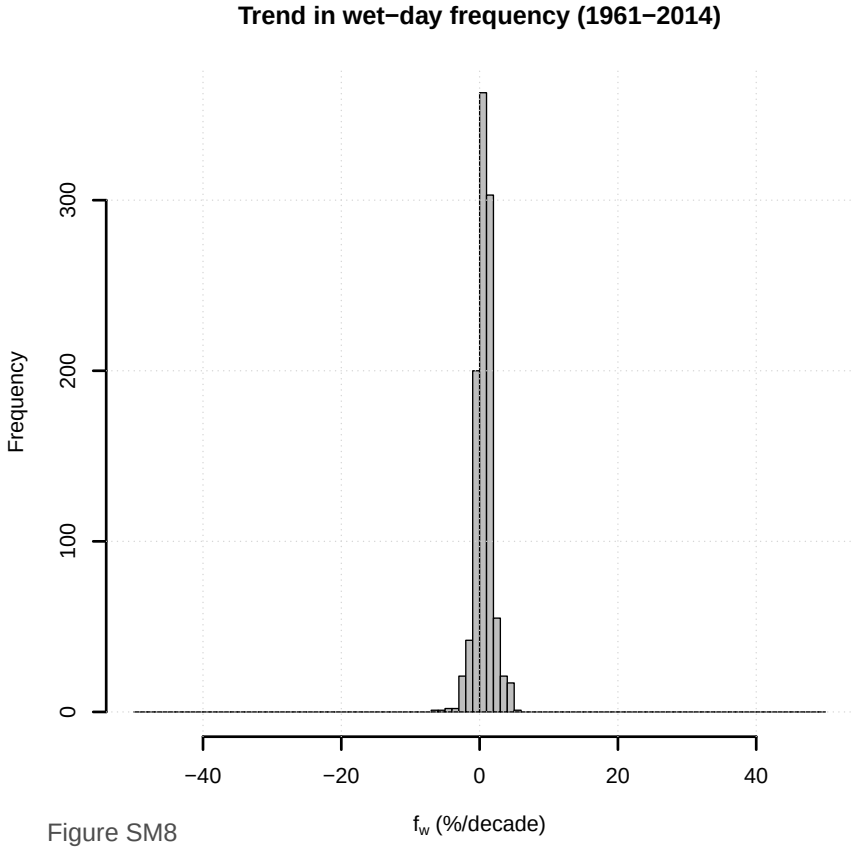

Figure SM8

Figure S8. Trend estimates of the wet-day frequency f_w for the 1032 locations for the period 1961-2014 suggests values scattered around zero. The cluster of trend values around zero is consistent with the annual wet-day frequency being stationary, but there are regions with significant trends (Figure S9).

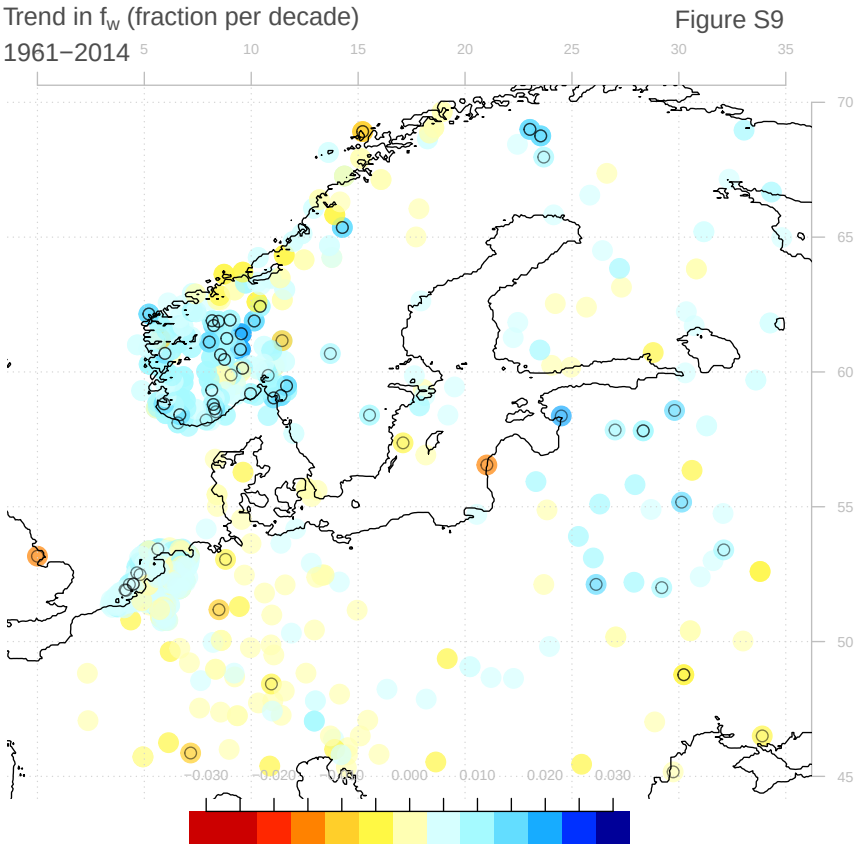

Figure S9. Map of the historical trends in the wet-day frequency f_w for the period 1961-2014. There has been a general increase in the number of wet-days in southern Scandinavia but otherwise no coherent pattern.

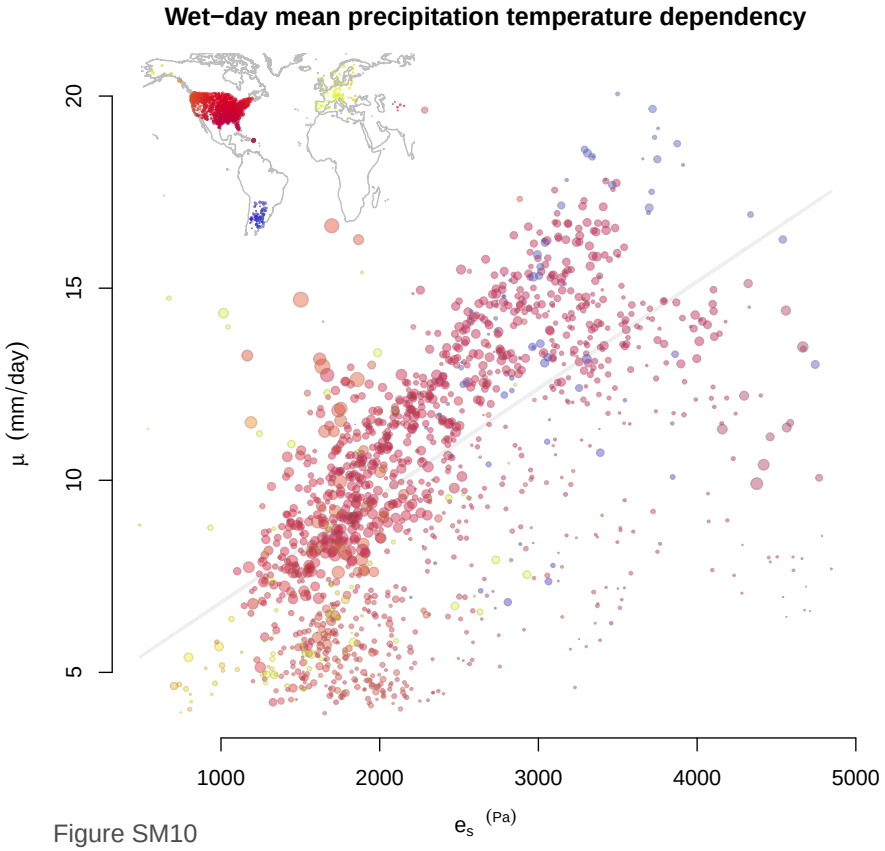

Figure SM10

Figure S10. Scatter plot showing the correlation between the climatological mean daily maximum temperature (converted to saturation vapour pressure) and the wet-day mean μ. The size of the symbols is proportional to the number of rainy days. The inset shows locations of stations used to compare the climatological mean wet-day mean against the mean surface temperature. The colours of symbols in the scatter plot match those in the map. The data included CLARIS data set from South America, a subset of the ECA&D in Europe used in the COST-VALUE experiment 1, and a subset of station data from GDCN as in Smith et al. (2015) but selecting the stations with the longest records. The selection of location was also limited to sites where both temperature and precipitation had been recorded. Only stations with more than 20000 valid data points were selected, and only the 1945–2015 period was used.

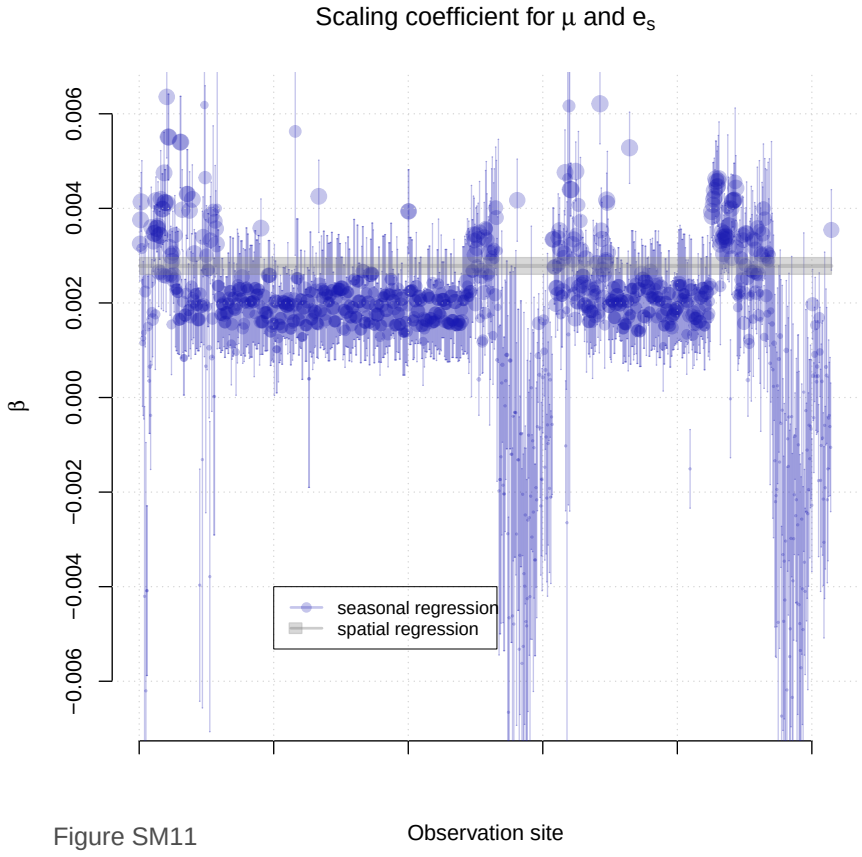

Figure SM11

Figure S11. Comparison between the regression coefficients estimated for each location based on the seasonal cycles in μ and e_s (blue) and based on the regression analysis of the mean climatology of μ and e_s at various stations in Europe, South America and North America as in Figure S10 (grey). Error bars represent two standard errors. The size of the symbols is proportional to the R^2 statistics from the regression analysis between the two mean seasonal cycles. The comparison between the results from the two types of analyses suggests a consistency within the margin of error for the locations where the mean seasonal cycle in μ matched that of the regionally averaged e_s in the predictor domain (Figure S2).